NOTICE CONCERNING COPYRIGHT RESTRICTIONS

Induced Seismicity Monitoring Tools for the Geothermal Environment

Mark Leidig[1], Delaine Reiter[1], Aaron Ferris[1], and William Rodi[2],

[1]Weston Geophysical Corp.
[2]Massachusetts Institute of Technology

Keywords

Geothermal, induced seismicity, enhanced geothermal systems (EGS), geophysics, injection, event detection, reservoir characterization

ABSTRACT

The monitoring of induced seismicity has become an important objective as geothermal and other energy production operations have moved closer to population areas. Fluids withdrawn from or injected into the subsurface cause changes in the local stress field, which can result in the generation of earthquakes, either on new or pre-existing faults. Examples of such earthquake activity include The Geysers geothermal field, where induced seismicity has occurred for decades, the 2008-2009 earthquake swarms near the Dallas/Ft. Worth airport, and the 2010-2011 earthquake swarms in central Arkansas, possibly including a magnitude 4.7 event. The latter two examples are likely attributed to fault reactivation from subsurface water injection.

The majority of seismic monitoring tools were developed for regional and teleseismic distances. Without adaptation, these tools are not well suited for the small-scale heterogeneity and the higher frequency content data observed at the reservoir scale. In order to monitor for and possibly prevent unwanted induced seismicity, it is necessary to develop new or adapt and refine existing tools.

An initial step in monitoring for induced seismicity is to develop a seismic velocity model. We have adapted a regional scale joint inversion technique that includes important reservoir scale features such as travel-time prediction methods that are not limited to layered structures or surface receivers and 3-D nonlinear velocity tomography with geostatistical constraints. To aid development of a starting model for the inversion, we investigated the use of a passive seismic technique known as seismic noise tomography, a method traditionally employed at regional distances to calibrate the velocity model between two stations.

We developed an event detection algorithm specifically designed to identify small seismic signals in noisy data. Event locations are then determined by a specially modified version of the Grid-Search Multiple Event Location (GMEL) software originally developed to locate nuclear testing around the world. In this paper, we present the development of this software and examples of its application on induced seismicity data sets.

Introduction

Seismic events that are related to human activities, such as fluid injection/withdrawal, dam building, mining, etc., are referred to as induced seismicity. Often the seismicity is intended and beneficial, as in the case of hydraulic stimulation for developing geothermal or oil/gas fields. We refer to this desired seismicity as stimulation induced seismicity. Cladouhos *et al.* (2010) denote any seismic activity related to fluid injection (either intended or not) as injection-induced seismicity (IIS) and explain how it occurs along with discussing a number of relevant examples. Some of the events in these examples were relatively large and could cause minor structural damage, placing them into a category we refer to as unintended induced seismicity (UIS).

One of the most significant UIS events for the geothermal industry was the magnitude 3.4 earthquake that occurred near Basel, Switzerland during stimulation of the reservoir for an enhanced geothermal system (EGS). Induced seismicity led to the cancellation of the project. Larger events have occurred in other geothermal fields, including The Geysers and Paradox Valley, but these areas are less inhabited so the consequences of induced seismicity are reduced.

Although the seismic activity in 2008-2009 near the Dallas/Ft. Worth airport and the 2010-2011 activity in central Arkansas are not associated with geothermal activity, these events occurred in close proximity and temporally to underground water injection, which should be of note to the geothermal community. Frohlich *et al.* (2011) suggest it is likely that injected fluids re-activated a fault below the DFW airport.

Regardless of the cause of the seismicity, detecting and locating any induced seismic events is important for field operators. Not only can a change in quantity or magnitude of events serve as a warning of an impending larger event, but observing the event

hypocenters over time can provide relevant information on the status of the field and size of the reservoir.

To extract more information on the properties and changes occurring in the reservoir, we have modified advanced detection and subsurface imaging tools, originally developed for the nuclear monitoring industry, to the reservoir scale. These tools model the seismic velocity structure through non-linear joint inversion of body and surface waves, and allow for the detection and location of seismic events. With the information provided by these tools, it is possible to produce time-varying images of the reservoir, illuminating regions where changes have occurred.

To illustrate the capabilities of the new event detection and location software, we processed the 11 precisely located seismic events from the DFW earthquake sequence reported on by Frohlich *et al.* (2011). We will refer to the Frohlich *et al.* event locations as the UT/SMU locations. For testing and development of the time-varying velocity modeling tools, we utilized data from The Geysers Calpine/Unocal seismic network. Seismic activity at The Geysers geothermal field has been recorded continuously for over a decade and makes an excellent data set for examining time variant geophysical changes.

Event Detection and Location

A fully automated detection and location system is an important feature for the geothermal industry as the number of seismic sensors and continuous recording over months or years makes exclusively human analysis impractical. We developed a new software package to automatically detect and locate seismic events, particularly with low signal-to-noise ratios. The detection portion of the software is based on the approach of Gibbons *et al.* (2008), which was designed to detect events at regional (200-2000 km) and teleseismic (>2000 km) distances, but we adapted the approach to the geothermal environment.

The detection methodology is well suited to small microseismic signals and/or high noise environments due to its analysis of the energy content of the waveform rather than the absolute waveform amplitudes, as is used by many traditional detection methods. Therefore, the magnitude threshold of detection can be reduced.

The automated detection software successfully identified all 11 earthquakes detailed in Frohlich *et al.* (2011). These events ranged in magnitude from 1.7 to 2.3 and were recorded by five surface three-component stations providing 220° of azimuthal coverage.

Automatic versus Analyst-Reviewed Phase Picks

In the automated detector, the data streams are read continuously, phase arrivals are detected, phase identification (i.e., P-wave or S-wave) is performed, and azimuth estimation is calculated. The detected arrivals are then associated with specific events via a method similar to generalized beamforming (Ringdal and Kvaerna, 1989), which is the time shifting and stacking of individual waveforms based on a proposed event location.

This information is then either sent to the location algorithm or an analyst can verify and adjust the arrival data, if needed. This processing flow allows an initial event detection and location to be made prior to an analyst examining the data and refining the location, thereby significantly reducing the analyst work load.

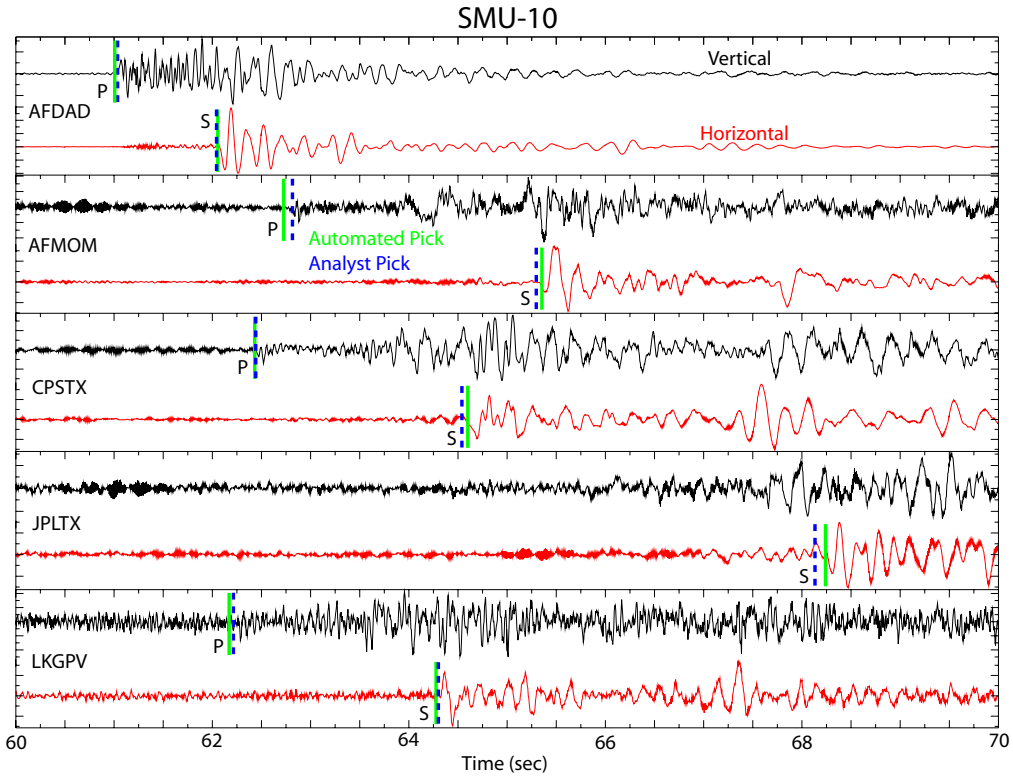

Figure 1. Comparison of automated (green solid line) and analyst (blue dashed line) phase arrival picks for DFW earthquake SMU-10. For the five recording stations, the vertical component (black) and one horizontal component (red) are plotted, with the P-wave picks shown on the vertical component and the S-wave picks shown on the horizontal component.

Figure 1 shows a comparison of the fully-automated and analyst-reviewed picks for event SMU-10 from the DFW earthquake sequence. Typically, the automated picks are within 0.1 seconds of the best analyst picks even for higher noise recordings, such as at station LKGPV. This arrival difference is only slightly larger than the error that would be placed on the human analyst picks.

Event Locations

The event location is determined using the Grid-search Multiple-Event Location (GMEL) technique. GMEL uses the observed arrival times to compute event locations and their associated uncertainty regions (Rodi, 2006). GMEL was originally developed to address the difficult problem of accurately locating events that are sparsely observed at regional and/or teleseismic distances,

such as in the nuclear test monitoring problem, but a version of this software was modified for the geothermal environment.

We solved for the earthquake locations with GMEL and the flat layer velocity model described in Frohlich *et al.* (2011) using the fully-automated phase picks and again with the analyst-reviewed phase picks. Figure 2 shows that the event locations with analyst picks have less scatter and are closer to the UT/SMU locations than the locations with the fully-automated picks. Although the automatic locations do not provide the best location estimates, they provide a good preliminary location prior to an analyst reviewing the event parameters. Most importantly, the automatic locations alert the operator that an event has occurred. After analyst review, the location errors are reduced and the GMEL event locations cluster around the UT/SMU locations, indicating the same linear NNE/SSW epicenter trend.

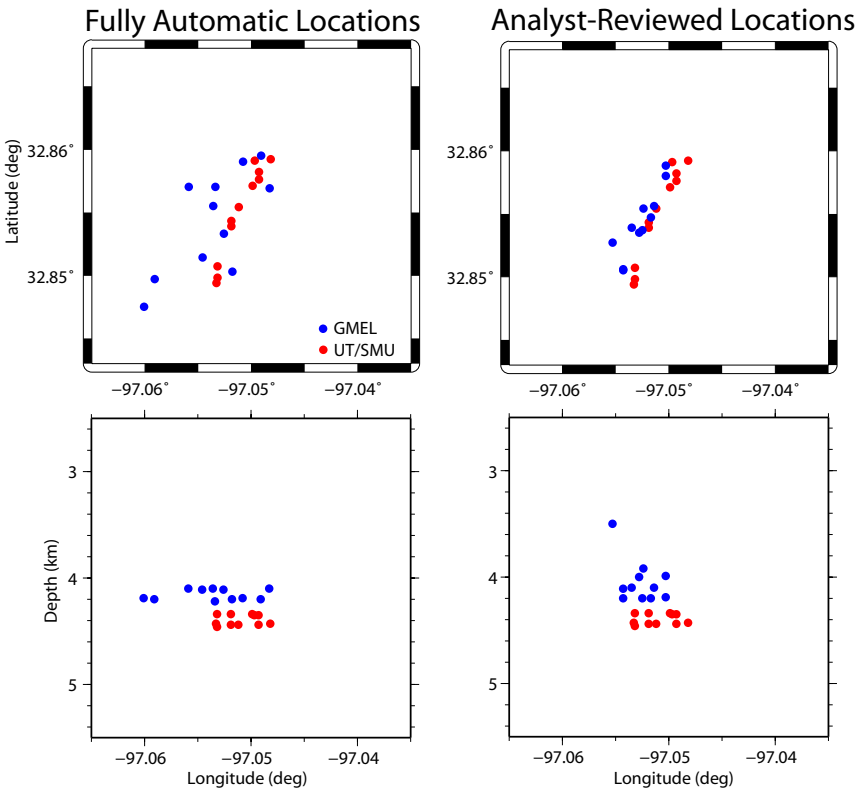

Figure 2. Earthquake location plots for the fully automatic processing (left) and analyst-reviewed processing (right). The top row shows the locations in map view, and the bottom row shows the locations in depth cross-sections. The red dots are the UT/SMU locations, and the blue dots are the GMEL locations from this study.

The UT/SMU locations were calculated with a relative event location algorithm, while our locations were determined on an individual event basis. The GMEL software is also capable of performing a relative event location, but this is beyond the scope of this paper. The difference in location methodology and/or velocity model may explain the small systematic difference observed in the UT/SMU and GMEL event depths.

We recognize that the exact hypocenter locations of the DFW events are a sensitive matter. Our locations presented in this paper should not be construed as contradictory to the UT/SMU locations in any way. The UT/SMU locations were carefully derived by analysts performing numerous advanced computational methods on the data and ultimately performing a high resolution relative location procedure. We compare our locations to the UT/SMU locations purely to show the potential of our automatic event detection/location software. In fact, the GMEL locations substantiate the UT/SMU locations as we obtained very similar earthquake hypocenters utilizing a different approach.

4-D Seismic Velocity Models

To successfully monitor induced seismicity, scientists must be able to accurately track time-varying subsurface heterogeneity. To address these issues we are adapting advanced subsurface imaging techniques originally developed for seismic nuclear monitoring purposes to the local and reservoir scales. Our ultimate objective is to jointly invert body- and surface-wave data for seismic P and S velocity structure and improved event locations. These quantities are important for fracture monitoring and tracking of production changes in all types of shallow reservoirs.

Velocity Imaging Techniques

In general, our inversion software solves jointly for the subsurface P and S velocity structure, earthquake hypocenters, and origin times using combinations of body-wave and surface-wave data. The joint inversion method is based on a Bayesian framework (e.g. Tarantola, 2005) in which prior information on the unknown velocity parameters is specified in terms of velocity bounds, geostatistical parameters (prior variances and spatial correlation lengths), and a correlation coefficient that couples P-wave and shear-wave velocity variations. To solve the joint problem, we implement separate procedures for linearized travel-time and delay-time tomography, nonlinear inversion of surface-wave dispersion curves, and seismic event location. The travel-time tomography, applied to first-arriving P-wave data, updates the P velocity model, while the delay-time tomography and dispersion inversion together update the S velocity model. These procedures are repeated iteratively to handle the nonlinearity of the problem. However, in our reservoir-scale applications thus far, we have inverted only P-wave arrival times (omitting S-wave times and surface-wave data) and applied our inversion method in an "uncoupled" mode to estimate the P-velocity structure and event hypocenters.

To generate the predicted travel times needed by our P travel-time inversion algorithm, we currently use the Podvin-Lecomte (P-L) method (Podvin and Lecomte, 1991; Lomax *et al.*, 2000), which solves the first-arrival travel time problem in a 3-D medium using a finite-difference approximation of the eikonal equation and Huygens' Principle. In addition, we use the GMEL algorithm to relocate the events between successive iterations of the P travel-time inversion procedure.

To date we have applied our P travel-time inversion algorithm to a single year of seismic data from the 22-station Geysers seismic network in northern California. We note that we determined only a

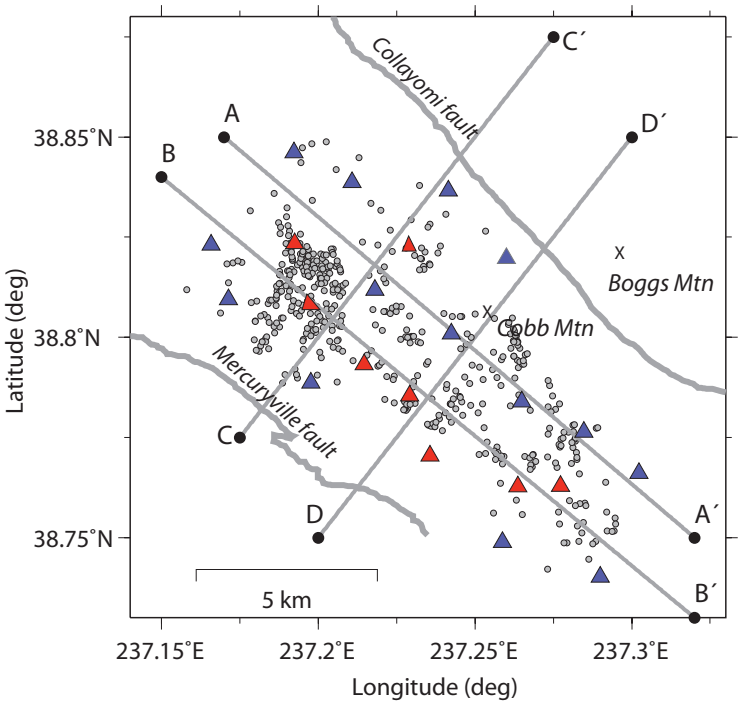

Figure 3. Map of The Geysers area with four tracks (A-A′, B-B′, C-C′, D-D′) that were used to slice through the final tomographic model shown in Figure 4a. The Geysers seismic network is shown with blue (vertical component) and red (3-component) triangles. Gray dots show the epicenters from the earthquake database utilized in the inversion.

"snap-shot" of the velocity structure based on data from a single year (2000). In general, our inversion method can be applied in a time-dependent manner to monitor changes in the velocity structure beneath a reservoir and the migration of seismicity patterns. In the following paragraphs we describe the application of our inversion method in The Geysers.

Application to Data from The Geysers

We retrieved a waveform data archive from The Geysers seismic network, which was initially deployed and operated by the Unocal Geothermal Division and is now provided through collaboration between the Calpine Corporation and the Northern California Earthquake Data Center (NCEDC). This data archive comprises over ten million waveforms recorded from tens of thousands of small earthquakes between 1989 and 2000. To generate an inversion database, we processed a subset of Geysers data from the year 2000. We constructed the P arrival database

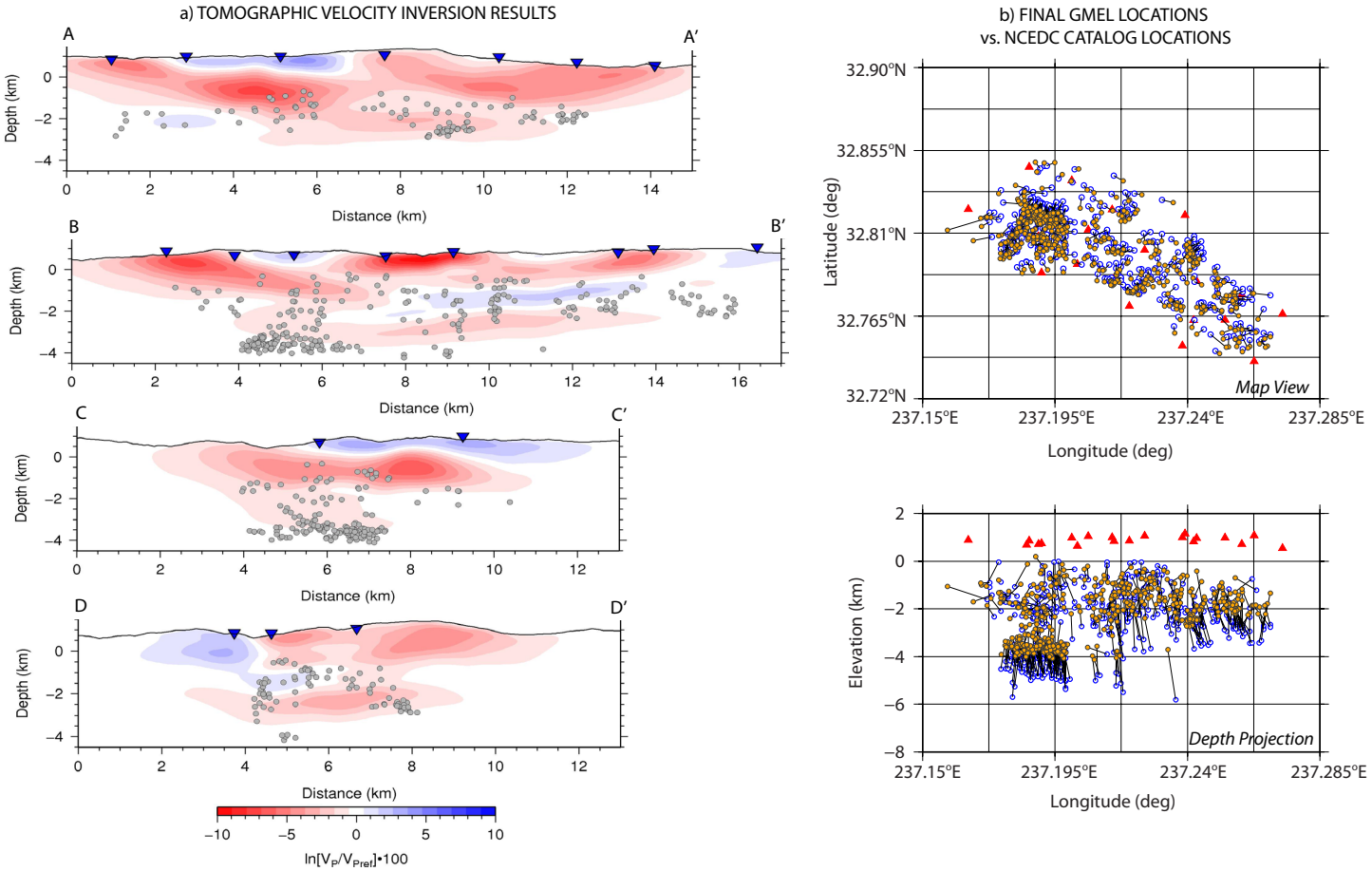

Figure 4a. Results from applying nonlinear P tomography to The Geysers P-arrival database. The model is displayed in percent variation from a 1-D linear gradient starting model. b) Comparison of starting model (blue circles) and final model (yellow circles) hypocenters found using the Weston/MIT velocity inversion/hypocenter location algorithm (top panel shows map view of epicenters, and bottom panel shows depth-projection view; in both subplots the red triangles depict the stations in The Geysers network).

by associating waveforms from the archive based on events published in the NCEDC catalog. Our final database contained 470 events, with 9,787 arrivals, after detection and association using standard techniques.

We applied the inversion method described in the previous section to our Geysers event database to estimate updated hypocenters and the P velocity structure in the station network region. The model region was chosen to cover a rectangular area between latitudes 38.7264°N and 38.8811°N, and longitudes 237.1364°E and 237.3310°E. The inversion velocity grid was sampled at a 400-m lateral spacing and at depths from -1.7 km (i.e. above the highest station elevation near Cobb Mountain) to 5.9 km in 200-m intervals. This translates to a grid of approximately 20 km by 15 km in north-south and east-west extent, respectively, and 7.6 km in depth. The travel-time grids calculated with the P-L method were generated at a much finer grid spacing (50 m) than the inversion model to ensure accuracy of the travel times and ray path sensitivities. We selected the starting velocity model for the inversion as a 1-D structure with constant-gradient layers, based on work published in previous studies and some simple regression analysis of the travel times in the arrival database.

We tested a variety of geostatistical parameters for stabilizing the inversion before selecting an 800-m lateral correlation length (2 nodes); a 200-m depth correlation length (1 depth node); and a prior model error of 5%. For event relocation, we assumed the bulletin locations have normally distributed errors with a prior standard deviation of 3.5 km on epicenter, 1 km on depth, and 0.5 seconds on origin time. The initial root-mean-square (RMS) fit to the travel times prior to relocation and velocity update was 0.33 seconds. For the first step of the inversion procedure, we relocated the events in the initial model, which significantly improved the RMS fit to the travel times to 0.053 seconds.

We applied three iterations of the nonlinear hypocenter/velocity inversion algorithm, resulting in a final RMS fit to the travel times of 0.044 seconds (a total variance reduction of 86%). The final velocity structure with respect to the 1-D starting model is shown in Figure 4a, along depth sections marked by the A-A', B-B', C-C' and D-D' linear tracks pictured in Figure 3. Even though most of the RMS reduction is accomplished with the initial relocation in the 1-D starting model, the tomographic image in Figure 4a shows that the new velocity model has significant 3-D structure. The range in variation from the 1-D model is approximately -10% to +5%.

Conclusions

We have developed new tools that improve the ability to automatically detect and locate seismic events in the geothermal field. In addition, we are adapting seismic velocity imaging tools traditionally used at regional and teleseismic distances to the reservoir scale. The velocity imaging tools will not only allow better resolution of the geothermal reservoir and improve the seismic event locations, but will be capable of illuminating subsurface velocity changes in the field over time. Monitoring the seismic activity and tracking changes in the field will help operators produce their fields at optimal levels and possibly prevent unintended induced seismicity.

Acknowledgements

This work was funded under DOE Small Business Innovation Research grants DE-SC00004483 and DE-FG02-07ER84683.

References

Cladouhos, T., S. Petty, G. Foulger, B. Julian, and M. Fehler, 2010. "Injection induced seismicity and geothermal energy", *Geothermal Resources Council Trans.*, v. 34, p. 1213-1220.

Frohlich, C., C. Hayward, B. Stump, and E. Potter, 2011. "The Dallas–Fort Worth earthquake sequence: October 2008 through May 2009", *Bull. Seism. Soc. Am*., v. 101, p. 327-340.

Gibbons, S. J., F. Ringdal, and T. Kvaerna, 2008. "Detection and characterization of seismic phases using continuous spectral estimation on incoherent and partially coherent arrays", *Geophys. J. Int.*, v. 172, p. 405-421.

Lomax, A., J. Virieux, P. Volant, and C. Berge, 2000. "Probabilistic earthquake location in 3D and layered models: Introduction of a Metropolis-Gibbs method and comparison with linear locations", *in* C. H. Thurber and N. Rabinowitz, eds., *Advances in Seismic Event Location*, Kluwer, Amsterdam, p. 101–134.

Podvin, P., and I. Lecomte, 1991. "Finite difference computation of travel times in very contrasted velocity models: a massively parallel approach and its associated tools", *Geophys. J. Int.*, v. 105, p. 271–284.

Ringdal, F., and T. Kvaerna, 1989. "A multi-channel processing approach to real time network detection, phase association, and threshold monitoring", *Bull. Seism. Soc. Am*., v. 79, p. 1927-1940.

Rodi, W., 2006. "Grid-search event location with non-Gaussian error models", *Phys. Earth. Planet. Int.*, v. 158, p. 55-66.

Tarantola, A., 2005. "Inverse Problem Theory and Methods for Model Parameter Estimation:" Society for Industrial and Applied Mathematics.